Appl Microbiol Biotechnol (2015) 99:3093–3102
DOI 10.1007/s00253-014-6335-x

Probing C-terminal interactions of the *Pseudomonas stutzeri* cyanide-degrading CynD protein

Mary Abou-Nader Crum · Jason M. Park · Andani E. Mulelu · B. Trevor Sewell · Michael J. Benedik

Received: 18 August 2014 / Revised: 10 December 2014 / Accepted: 14 December 2014 / Published online: 31 December 2014

Abstract The cyanide dihydratases from *Bacillus pumilus* and *Pseudomonas stutzeri* share high amino acid sequence similarity throughout except for their highly divergent C-termini. However, deletion or exchange of the C-termini had different effects upon each enzyme. Here we extended previous studies and investigated how the C-terminus affects the activity and stability of three nitrilases, the cyanide dihydratases from *B. pumilus* ($CynD_{pum}$) and *P. stutzeri* ($CynD_{stut}$) and the cyanide hydratase from *Neurospora crassa*. Enzymes in which the C-terminal residues were deleted decreased in both activity and thermostability with increasing deletion lengths. However, $CynD_{stut}$ was more sensitive to such truncation than the other two enzymes. A domain of the *P. stutzeri* $CynD_{stut}$ C-terminus not found in the other enzymes, 306GERDST311, was shown to be necessary for functionality and explains the inactivity of the previously described $CynD_{stut\text{-}pum}$ hybrid. This suggests that the *B. pumilus* C-terminus, which lacks this motif, may have specific interactions elsewhere in the protein, preventing it from acting in trans on a heterologous CynD protein. We identify the dimerization interface A-surface region 195–206 (A2) from $CynD_{pum}$ as this interaction site. However, this A2 region did not rescue activity in C-terminally truncated $CynD_{stut}\Delta302$ or enhance the activity of full-length $CynD_{stut}$ and therefore does not act as a general stability motif.

Keywords Cyanide dihydratase · Nitrilase · Cyanide · Bioremediation

Introduction

The cyanide dihydratases are enzymes belonging to the nitrilase branch of the nitrilase superfamily (Pace and Brenner 2001). Nitrilases hydrolyze organic nitriles to carboxylic acids and ammonia under mild acidic or basic reaction conditions (Thimann and Mahadevan 1964), in this instance, cyanide to formic acid (Meyers et al. 1993). Although there are no crystal structures of members for any members of the nitrilase branch, there are structures of other members of the superfamily such as a DCase (*N*-carbamoyl-D-amino acid amidohydrolase) from *Agrobacterium* sp. strain KNK712 (Nakai et al. 2000), NitFhit (nit-fragile histidine triad fusion) protein from *Caenorhabditis elegans* (Pace et al. 2000), a putative cyanide hydrolase from *Saccharomyces cerevisiae* (Kumaran et al. 2003) as well as several amidases (Hung et al. 2007; Kimani et al. 2007).

Models have been proposed for several members of the nitrilase branch (Sewell et al. 2003; Thuku et al. 2009; Thuku et al. 2007) based on three-dimensional electron microscopy and the fitting of homology models obtained by alignment of sequences to related crystallographically determined structures. Members of the superfamily all possess similar monomer and dimer structures (Pace and Brenner 2001). The monomers fold into an αββα structure and then pair across the A surface to form αββα–αββα dimers. In the nitrilases, these dimers act as the building blocks for the

Electronic supplementary material The online version of this article (doi:10.1007/s00253-014-6335-x) contains supplementary material, which is available to authorized users.

M. A.-N. Crum · J. M. Park · M. J. Benedik (✉)
Department of Biology, Texas A&M University, College Station, TX 77843-3258, USA
e-mail: benedik@tamu.edu

A. E. Mulelu · B. T. Sewell
Structural Biology Research Unit, Division of Medical Biochemistry, Institute of Infectious Disease and Molecular Medicine, University of Cape Town, Cape Town, South Africa

formation of left-handed, spiral oligomers by interacting at the C surface. The spiral oligomers of CynD from *Pseudomonas stutzeri* AK47 or *Bacillus subtilis* C1 comprise 14 or 18 monomers, respectively (Jandhyala et al. 2003; Sewell et al. 2003), under near-physiological conditions.

One notable difference between the sequences occurs at the carboxy-terminus (Fig. S1). The microbial nitrilases from *B. pumilus* (Jandhyala et al. 2003), *P. stutzeri* (Sewell et al. 2003), *Neurospora crassa*, *Gloeocercospora sorghi*, and other microbes (Basile et al. 2008) and the crystalline amidases from *Helicobacter pylori* (Hung et al. 2007), *Geobacillus pallidus* (Agarkar et al. 2006; Kimani et al. 2007), and *Pseudomonas aeruginosa* (Andrade et al. 2007a; Andrade et al. 2007b) all have an extension of their C-terminus relative to many members of the superfamily. This extension varies in length as well as in sequence, with no preserved similarity even among closely related enzymes, as well as no preserved predicted secondary structure (Thuku et al. 2009).

The crystal structures of the amidases show that the carboxy terminal extension contributes substantially to the A surface as well as the other associating surface in the "trimer of dimers" hexameric structure. In the case of the amidases, the carboxy terminus is located on the outside of the hexameric assembly, but in the case of the spiral nitrilases, homology modeling locates the carboxy terminal on the inside of the spiral. Thus, the role or potential interactions in this region may not be strictly analogous.

Several studies point to the importance of the C-terminus. The nitrilase from *Rhodococcus rhodochrous* J1 is normally found as inactive dimers (Nagasawa et al. 2000) (Stevenson et al. 1992). Following post-translational processing that removed 39 C-terminal amino acids, the enzyme formed stable active helices (Thuku et al. 2007). This natural process is thought to be autocatalyzed. Genetic deletions of more (50aa) or fewer (27aa) than the 39 residues led to formation of inactive "c"-shaped aggregates, thus implying that this region is important for the oligomerization and subsequent activity of the enzyme. Similar observations were noted with C-terminal deletions of an arylacetonitrilase from *Pseudomonas fluorescens* EBC191 (Kiziak et al. 2007).

The very similar cyanide dihydratases from *B. pumilus* C1 ($CynD_{pum}$) and *P. stutzeri* ($CynD_{stut}$) also show a significant difference in sequence and behavior of their C-termini. Alignment of $CynD_{pum}$ (330 aa) and $CynD_{stut}$ (334 aa) protein sequences reveals over 80 % identity for the first 300 residues but only 25 % for the C-terminal region. Truncations of their C-termini yielded discrepant results for the two enzymes (Sewell et al. 2005). $CynD_{pum}$ could tolerate truncation to residue 303 ($CynD_{pum}$ Δ303) and retain apparently normal activity; further deletion to residue 293 yielded protein with partial activity and deletion beyond that point rendered the enzyme inactive. In contrast, $CynD_{stut}$ became inactive with a deletion to 310. The same study also described the creation of hybrid enzymes where the C-terminus of $CynD_{pum}$ was replaced with that from $CynD_{stut}$, which yielded an active hybrid enzyme ($CynD_{pum\text{-}stut}$); however, the converse hybrid ($CynD_{stut\text{-}pum}$) had no detectable activity.

Participation of the C-terminus in oligomerization is seen in some structures from superfamily members that have extended C-termini. The C-terminus of amidase from *G. pallidus* folds into interlocking alpha helixes at the A surface (Kimani et al. 2007). Based on the amidase structure, modeling of the C-terminus in CHT from *N. crassa* suggests that C-terminus may also participate in oligomerization at the C surface (Dent et al. 2009). Although not as extended as the C-termini in the nitrilase and amidase sequences, the C-terminus in the structure of the C-shaped β-alanine synthase (βaS) from *D. melanogaster* interacts with the A surface and then is anchored at its C surface (Lundgren et al. 2008).

This study aims to further explore the role of the C-terminus in determining the stability and the activity of these enzymes and to better explain the results of the hybrids with interchanged C-termini.

Materials and methods

Culture media and reagents

All strains were grown in LB broth or plates with antibiotics at concentrations of 100 μg /ml of ampicillin, 25 μg/ml of kanamycin, or 25 μg/ml of chloramphenicol added as needed.

Bacterial strains and plasmids

E. coli strain MB3436 [Δ*endA thiA hsdR17 supE44 lacI*^{q} *ZΔM15*] was the host strain for DNA manipulations and expression of protein from pBC vectors and *E. coli* strain MB1837 [BL21 (DE3) pLysS] for protein expression from pET vectors. A synthetic gene encoding the *P. stutzeri* cyanide dihydratase but with *E. coli* optimized codons and additional restriction sites was used (Genbank KM459551). Plasmids are described in Table S1.

C-terminal amino acids deletion

Nitrilase alleles with deletions in their C-termini were constructed using Phusion High-Fidelity PCR Master Mix (New England Biolabs) and the primers listed in Table S2. The primers were designed to incorporate a stop codon at the desired position along with deletion of the coding region beyond to avoid any read-through expression of the wild-type protein. The mutations were confirmed by DNA sequencing.

Hybrid constructs

The *Bst*BI restriction site was introduced in cht_{cras}, $cynD_{pum}$ and $cynD_{stut}$ at nucleotides position 903, 858, 855 respectively which represent identical positions based on protein alignments. C-terminal swaps were constructed using this *Bst*BI site and an *Xho*I site at the end of each gene as described previously (Sewell et al. 2005). Hybrids are named designating the N-terminal region followed by the C-terminal, so for example, $CynD_{pum\text{-}stut}$ would represent the body of the enzyme from *B. pumilus* and the C-terminus from *P. stutzeri*.

Mutagenesis

In order to introduce different mutations in the C-terminal region of the $CynD_{stut\text{-}pum}$ and the $CynD_{stut\text{-}cras}$ hybrids, the C-terminal sequence was divided into three parts, beginning with the *Bst*BI restriction site mentioned above. Then three sets of overlapping oligonucleotides were annealed to reconstitute the C-terminal domain and introduced by restriction digestion and ligation. A list describing the DNA oligonucleotides and their sequences is shown in Table S3.

Site-directed mutagenesis reactions were carried out using 25 μl Phusion High-Fidelity PCR Master Mix with HF Buffer (New England Biolabs), 150 ng dsDNA template, and 100 ng of each of the forward and reverse primers. MQH_2O was added to the reaction mixture for a total volume of 50 μl. Each reaction was run for 18 cycles. The mutagenic primers are listed in Table S4. The mutations were confirmed by DNA sequencing.

For alanine scanning, overlapping primers were used to reconstitute the $CynD_{stut}$ C-terminus with mutations G306A, E307A, R308A, D309A, S310S, or T311A. The different primers and their sequences are listed in Table S5.

Substitution of the A and C surface regions in $CynD_{stut}$ for the $CynD_{pum}$ sequence was done by overlap extension PCR using the primers listed in Table S6. The products of these reactions were cloned into pBC-SKII+ between *Xba*I and *Xho*I.

Activity and stability measurements of deletion mutants

Overnight cultures of BL21 (DE3) cells transformed with each expression plasmid were diluted 1:100 in 3 ml LB kanamycin and grown to an OD600 of 0.3 at 37 °C. IPTG was added to 1 mM for induction, and incubation continued for 3–4 h at 30 °C. One milliliter of cells carrying wild-type or variant alleles was diluted to an OD600 of 0.3, and 200 μl was added to 800 μl of 50 mM MOPS, pH 7.7. Cyanide was added to 4 mM, and the reaction was maintained at room temperature; a 100-μl aliquot was removed every 2 min and the reaction terminated by adding 100 μl of picric acid reagent (0.5 % picric acid in 0.25 M sodium carbonate), incubated at 100 °C in a dry block for 5 min to allow color development, and the absorbance was measured at 540 nm. Routine enzyme activity was measured similarly but incubating for a single 30-min time point at room temperature.

To test stability, the cells were lysed at room temperature with B-PER II Protein Extraction Reagent (Thermo Scientific). Two milliliters of B-PER II reagent per gram of cell pellet was used, supplemented with 0.5 mg/ml lysozyme, 10 μg/ml DNase, and 1X EDTA-free protease inhibitors as recommended by the manufacturer. The cell lysate was centrifuged at 13,000 rpm for 15 min at 4 °C, and 80 μl of each lysate was resuspended in 4 ml of 50 mM MOPS, pH 7.7; the tubes were placed in a water bath at 38 °C (CynD) or 42 °C(CHT). At different time points, 0.5-ml aliquots were removed into new 1.5-ml microcentrifuge tubes and left to equilibrate at room temperature for 3 min before adding cyanide to a final concentration of 4 mM. The reaction was continued at room temperature, and the activity was monitored for the first 5 min with time points taken every minute. Ammonia production was measured by using Nessler reagent (Nichols and Willits 1934) and measuring absorbance at 420 nm for $CynD_{pum}$, $CynD_{pum}\Delta303$, $CynD_{stut}$, and $CynD_{stut}\Delta330$, whereas a picric acid assay (Jandhyala et al. 2005) was used to measure cyanide degradation by cyanide hydratases CHT_{cras} and $CHT_{cras}\Delta339$, which do not produce ammonia. Ammonia production and cyanide loss are co-linear, but ammonia production can be measured more accurately at early reaction times when using purified enzyme. Cell extracts contain substantial amounts of ammonia requiring the use of the cyanide loss (picric acid) assay, but with this assay one can only measure cyanide loss accurately when significant levels are degraded (greater than 10 %). With pure enzyme, one can readily measure the appearance of very low levels of ammonia, permitting accurate measurements at early reaction points, but only to be used with a purified enzyme.

Activity and stability measurements of $CynD_{stut}$ alanine mutants

Wild-type $CynD_{stut}$ along with the alanine mutants was grown in LB kanamycin and induced as described above. Cells were adjusted to a similar OD600 of 0.3, and 200 μl was added to 800 μl of 50 mM MOPS, pH 7.7, and cyanide was added to 4 mM and incubated at room temperature. At each time point, 100 μl of the reaction mixture was removed and combined in a 1.5-ml microcentrifuge tube with 100 μl picric acid reagent and incubated on a heat block at 100 °C for 5 min to allow color development. Then, 100 μl of the mixture was transferred into a 96-well plate, and absorbance was determined at OD 540 nm using a Benchmark Plus microplate reader (BioRad). The reaction rate of the mutants was then compared to wild-type $CynD_{stut}$. The stability test was performed as described above using cleared cell lysates; 80 μl of lysate

was added to 4 ml of 0.1 M MOPS, pH 7.7, and placed in a water bath at 39 °C. For each time point, 500 μl of the mixture was removed, to which 4 mM cyanide was added, and ammonia production was monitored as above.

Activity of A and C surface mutants in $CynD_{stut}$, $CynD_{stut}\Delta302$, and $CynD_{stut\text{-}pum}$

The active oligomer surface mutant in the $CynD_{stut\text{-}pum}$ background did not tolerate over-expression, so activity was tested from non-induced pBC constructs. MB3436 cells were freshly transformed with pBC-based plasmids, and cultures were inoculated from the single colonies and allowed to grow to saturation without induction. Activities of the CynD mutants were measured as follows: 50 μl of 6 mM KCN in 0.1 M MOPS (pH7.7) was added to 50 μl of culture in 1.5-ml microcentrifuge tubes. Reactions were terminated after 20 min with 100 μl of picric acid reagent (0.5 % picric acid in 0.25 M sodium carbonate). The tubes were incubated on a 100 °C heating block for 5 min. Then, 100 μl of the mixture was then transferred into a 96-well plate, and absorbance was determined at OD 540 nm using a Benchmark Plus microplate reader (BioRad).

Calculation of $\Delta\Delta G^*$ in the case of the active CynD and CHT mutants

A quantitative estimate of the thermostability of the active enzymes was obtained by calculating the differences in the activation energy for thermally induced activity loss between the wild type and the mutants ($\Delta\Delta G^*$). The measurement of kinetic stability of the proteins was done as describe above.

The rate of thermal inactivation, k_d, was obtained for both the wild type and the mutant enzymes from the slope of the graph of ln (% residual activity) versus t, where t is the time of incubation. The observed deactivation rate constant, k_d, can be related to ΔG^*, the activation energy, by the Arrhenius equation: $k_d = Ae^{-(\Delta G^*/RT)}$ where R is the gas constant and T is the absolute temperature at which the experiment is done. Hence, $\Delta\Delta G^* = \Delta G^*_{wt} - \Delta G^*_{mut} = RT \ln(k_{wt}/k_{mut})$. Negative values indicate that the mutant is less thermostable than the wild-type enzyme.

Protein purification and size exclusion chromatography

His-tagged $CynD_{stut}$ and $CynD_{stut}A2_{pum}$ in pET 28 were expressed and purified as previously described (Park 2014). The relative sizes of the $CynD_{stut}$ oligomers were measured by gel filtration. Protein samples were prepared in 0.1 M MOPS, pH 7.7, and separated on a Superdex™ 200 10/300 GL column (Amersham Biosciences; Uppsala, Sweden) at 0.5 ml/min equilibrated with 0.1 M MOPS, pH 7.7, using a BioRad BioLogic DuoFlow® HPLC.

Results

Effect of C-terminal deletions on nitrilase activity

A previous study looked at the effect of mutating interfacial residues on nitrilase activity, including deletions in the C-terminal region of two cyanide dihydratases, $CynD_{pum}$ and $CynD_{stut}$ (Sewell et al. 2005). Despite their high amino acid sequence identity, the two enzymes differed dramatically in their tolerance to C-terminal truncation, with $CynD_{pum}$ being notably more tolerant. This protein retained normal activity when deleted to 303 and partial activity at 293, whereas $CynD_{stut}$ lost all activity with similar deletions.

To extend this study to cyanide hydratase (CHT), similar-length truncations in CHT_{cras} (352aa) were created after residues 339, 323, and 307. Residue 307 is the position where the alignment with the bacterial CynDs diverges and aligns with residue 293 of *B. pumilus* CynD. Residue 323 is the position where the *N. crassa* CHT begins to diverge from other cyanide hydratases, such as the CHT of *G. sorghi*. One further deletion site was chosen randomly at residue 339. Two additional truncations were also constructed in *P. stutzeri*, at residues 330 and 310. $CynD_{stut}$ is normally 334 aa in length with a C-terminus 5 aa longer than $CynD_{pum}$. Although $CynD_{stut}\Delta310$ was previously described (Sewell et al. 2005), it was reconstructed for this work by creating a stop codon with subsequent removal of the remaining ORF, which existed in the prior construct, to avoid read-through.

Not surprisingly, all three enzyme activities declined with the deletions of increased size (Table 1). Similar to previous results (Sewell et al. 2005), $CynD_{pum}\Delta303$ retained about 87 % of wild-type activity; this decreased to 27 % when 39 amino acids were deleted ($CynD_{pum}\Delta293$), and no activity was observed with a larger deletion ($CynD_{pum}\Delta279$). In contrast, the *P. stutzeri* enzyme only tolerated the shortest deletion of five residues; a longer deletion to 310 decreased activity to about 13 %, and deletion to 302 abolished all activity. The CHT enzyme from *N. crassa* was somewhat intermediate and tolerated C-terminal deletions better than *P. stutzeri* but not as robustly as *B. pumilus* with respect to the length of deletion (Table 1).

Effect of C-terminal deletions on stability

Wang et al. (2012) identified CynDpum Q322R and E327G as mutations near the C-terminus that contributed to enhancing the pH stability of the enzyme, suggesting that the C-terminus played a role in conferring stability. This raises the possibility that in those cases in which the C-terminal truncated enzyme retained activity, a consequence of the truncation might be reduced stability. Using survival at elevated temperature as our assay, the two active mutants of $CynD_{pum}$ were probed: $CynD_{pum}\Delta303$, which although nearly wild type in activity

Table 1 Loss of cyanide-degrading activity upon C-terminal deletion of CynD and CHT

Mutant	Length of deletion (amino acids)	% of parental wild type (ΔA_{540}/min)
B. pumilus		
Δ303	28	87±5 (.037)
Δ293	38	27±2 (.012)
Δ279	52	Undetectable
P. stutzeri		
Δ330	5	97±3 (.10)
Δ310	26	13±5 (.015)
Δ302	33	Undetectable
N. crassa		
Δ339	13	46±8 (.09)
Δ323	29	22±5 (.040)
Δ307	45	Undetectable

Proteins were expressed from constructs in pET26b in strain MB1837 cells. The cyanide-degrading activity from whole cells was measured using 4 mM cyanide in 0.1 M MOPS at pH 7.7 at room temperature after 30 min of incubation. The remaining cyanide was determined using the picric acid assay, and the value for each mutant is presented relative to its wild-type parent and represents the average and the standard deviation from three separate samples. The average ΔA_{540}/min for each mutant is shown in parentheses

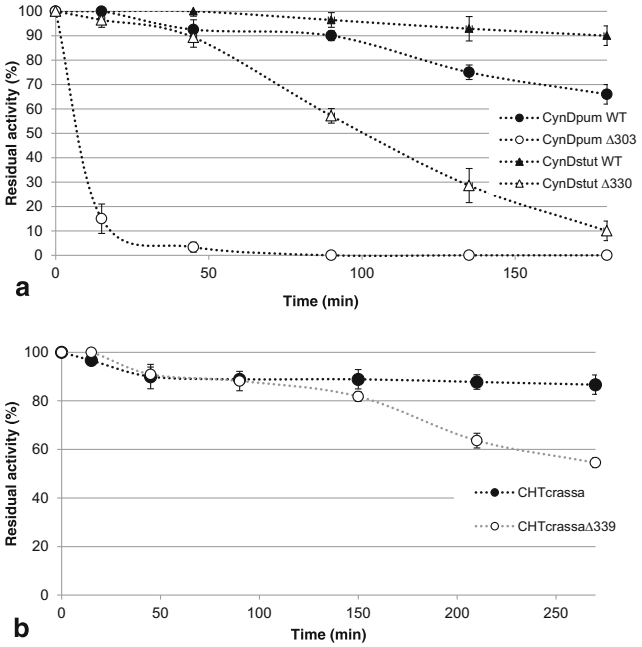

Fig. 1 Effect of C-terminal deletions on nitrilase stability. **a** $CynD_{pum}$ and $CynD_{stut}$ stability. Cleared cell lysates with protease inhibitor were incubated in a water bath at 38 °C, and at different times the remaining enzyme activity was tested. **b** CHT_{cras} stability. Residual activity was tested at room temperature after cleared cell lysates were incubated at 42 °C for the designated times. *Error bars* indicate the standard deviation of the average from three separate experiments

was very unstable, losing 85 % of its initial activity after 15 min of incubation at 38 °C (Fig. 1a), conditions where the wild type retained 100 %. Similar but not as dramatic results were seen with the 5aa deletion of $CynD_{stut,}$ Δ330: after 90 min of incubation at 38 °C, the mutant lost about 50 % of its initial activity (Fig. 1a), where the wild type only lost 5 %. $CynD_{pum}$ Δ303 and $CynD_{stut,}$ Δ330 displayed negative $\Delta\Delta G$ of −10.3 and −7.8, respectively, confirming their reduction in stability relative to their respective wild types (Table 2).

In contrast, CHT_{cras} Δ339 seemed to be more stable than deletions of the bacterial nitrilases. It was indistinguishable from wild type at 38 °C (data not shown), and only at 42 °C was a difference detectable with the deletion enzyme retaining nearly 60 % of initial activity after 3 h of incubation at 42 °C (Fig. 1b); it displayed a positive $\Delta\Delta G$ of 0.2, which indicates a slight increase in stability relative to the wild type (Table 2).

Heterologous C-terminal domains

Sewell et al. (2005) described the construction of CynD hybrids between $CynD_{pum}$ and $CynD_{stut}$. The $CynD_{pum\text{-}stut}$ hybrid carried the N-terminal body of $CynD_{pum}$ with its C-terminus replaced by that of $CynD_{stut}$ after position 286. This enzyme retained normal activity, whereas the converse $CynD_{stut\text{-}pum}$ hybrid had no detectable activity.

Shown in Table 3 is the activity of additional CynD and CHT hybrids; again $CynD_{stut}$ but also CHT_{cras} failed to have activity with a heterologous C-terminus, whereas $CynD_{pum}$ was tolerant to any C-terminal domain, not unexpected since it was also tolerant to deletion. It is important to note that the

Table 2 Thermostability of CynD and CHT mutants expressed as $\Delta\Delta G^*$

Mutant	Incubation temperature (°C)	$\Delta\Delta G^*$ (kJ/mol)
B. pumilus		
Δ303	38	−10.3
P. stutzeri		
Δ330	38	−7.8
G306A	39	−11.9
E307A	39	−2.7
R308A	39	−8.7
D309A	39	−8.3
S310A	39	−1.5
T311A	39	−7.6
N. crassa		
Δ339	42	0.2

Cleared cell lysates were incubated at various temperatures in a water bath, and the residual activity was tested at multiple time points (Fig. 1) by detecting ammonia production. Using the residual activity values, the differences in activation energy of thermal unfolding between the wild type and the mutants ($\Delta\Delta G^*$) were calculated as described in "Materials and methods"

$CynD_{pum}$ was unable to tolerate deletions to residue 286, so the heterologous C-termini do play some necessary role.

C-terminal residues required for $CynD_{stut}$ activity

The inability of the *P. stutzeri* CynD to tolerate deletion or a heterologous C-terminus suggests that residues specific to the $CynD_{stut}$ C-terminus are necessary for its activity but are missing and not necessary for $CynD_{pum}$. Although the C-terminal sequences are highly dissimilar, we aligned the $CynD_{pum}$ and $CynD_{stut}$ and compared amino acid side chain properties (Fig. S2). Two regions that stand out as notably different are 306GERDST and 320LSVSDEEPV found in the *P. stutzeri* enzyme but missing in that of *B. pumilus*.

The inactive $CynD_{stut\text{-}pum}$ hybrid was used as a platform to test whether either of these sequences of amino acids was sufficient to restore activity. The residues GERDST were introduced at position 306 to 311, residues VSDE at position 322 to 325, and residues LSVSDEEPV at position 320 to 328. The cyanide-degrading activity of $CynD_{stut\text{-}pum}$ carrying each was then tested (Table 4).

Restoring amino acids 306GERDST311 to the $CynD_{stut\text{-}pum}$ hybrid partially rescued the activity of the enzyme to about 30 % of wild-type $CynD_{stut}$ (Fig. 2); however, neither 322VSDE325 nor 320LSVSDEEPV328 had any effect. The properties of the enzyme containing both substitutions, $CynD_{stut\text{-}pum}$ 306GERDST311/322VSDE325, were indistinguishable from $CynD_{stut\text{-}pum}$ 306GERDST311 (Fig. 2).

As confirmation, the GERDST domain in the active $CynD_{stut\text{-}pum}$ 306GERDST311 was restored back to NHQKNE, and the protein lost its activity again (Tables 4 and 5). These results suggest that some or all of the 306GERDST region is required for activity (albeit partial Fig. 2) of the $CynD_{stut\text{-}pum}$ hybrid and presumably of $CynD_{stut}$.

Surprisingly, activity was observed in whole cells but was rapidly lost in cell lysates. This might indicate a rapid unfolding or aggregation of the mutant hybrids once the cells are lysed or perhaps increased susceptibility to proteolysis.

Table 3 Cyanide-degrading activity of hybrid nitrilases where C-terminus was exchanged

Hybrid	Residues	% of parental wild type (ΔA_{540}/min)
$CynD_{pum\text{-}stut}$	Residues1-286 from *B. pumilus*, 287-end from *P. stutzeri*	103±3 (.045)
$CynD_{pum\text{-}cras}$	Residues1-286 from *B. pumilus*, 287-end from *N. crassa*	59±2 (.025)
$CynD_{stut\text{-}pum}$	Residues 1–287 from *P. stutzeri*, 288-end from *B. pumilus*	Undetectable
$CynD_{stut\text{-}cras}$	Residues 1–287 from *P. stutzeri*, 288-end from *N. crassa*	Undetectable
$CHT_{cras\text{-}stut}$	Residues 1–303 from *N. crassa*, 304-end from *P. stutzeri*	Undetectable
$CHT_{cras\text{-}pum}$	Residues 1–303 from *N. crassa*, 304-end from *B. pumilus*	Undetectable

The activity was tested as in Table 1 from whole cells. Activity is presented as a percentage relative to the wild type (the wild type is the parent enzyme defined by the ~300-residue N-terminal domain) with ΔA_{540}/min presented in parentheses

Table 4 Activity of $CynD_{stut\text{-}pum}$ hybrids and mutants

Hybrid	Mutation	% of wild type (ΔA_{540}/min)
$CynD_{stut}$	Wild type	100 % (0.186)
$CynD_{stut\text{-}pum}$	Hybrid	Undetectable
$CynD_{stut\text{-}pum}$ GERDST	306NHQKNE→306GERDST	33 %±3 (0.062)
$CynD_{stut\text{-}pum}$ VSDE	322HGIL→322VSDE	Undetectable
$CynD_{stut\text{-}pum}$ LSVSDEEPV	320YQHGILEEK→320LSVSDEEP	Undetectable
$CynD_{stut\text{-}pum}$ NHQKNE	306GERDST→306NHQKNE	Undetectable
$CynD_{stut\text{-}pum}$ N*DKE*NE	H307D Q308K K309E	Undetectable
$CynD_{stut\text{-}pum}$ *GHR*KN*T*	N306G Q308R E311T	Undetectable
$CynD_{stut\text{-}pum}$ *GHQD*NE	N306G K309D	Undetectable
$CynD_{stut\text{-}pum}$ *GE*QKNE	N306G H307E	10 %±4 (0.019)
$CynD_{stut\text{-}pum}$ N*E*QKNE	H307E	Undetectable

The activity was tested as in Table 1 from whole cells except that multiple time points were taken to more accurately measure low-activity mutants. Changes made to the parent sequence NHQKNE in $CynD_{stut\text{-}pum}$ are italicized

Alanine scanning of $CynD_{stut}$ GERDST region

Alanine scanning through the GERDST region in the wild-type $CynD_{stut}$ was performed, and the activity of each mutant

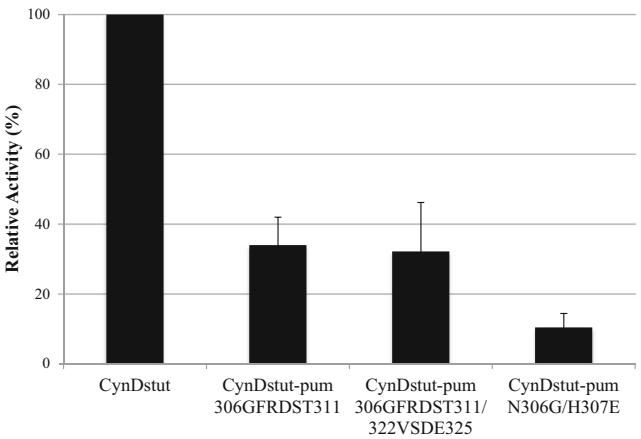

Fig. 2 Comparison of cyanide-degrading activity of $CynD_{stut\text{-}pum}$ tail substitutions. Cell cultures were adjusted to similar OD600 of 0.3, and cyanide degradation was monitored using the picric acid assay. The $CynD_{stut}$ wild type reaction rate was taken as 100 %, and the relative activity of the mutants was then calculated. *Error bars* indicate the standard deviation of the average from three experiments

Table 5 Partial restoration of $CynD_{stut\text{-}pum}$ activity by an oligomer surface region of $CynD_{pum}$

Hybrid	Mutation	Activity
$CynD_{stut}$	Wild type	100 % (0.24)
$CynD_{stut\text{-}pum}$ $C1_{pum}$	59-LGHPEYTRRFYHT-71 to IGHPEYTRKFYHE	Undetectable
$CynD_{stut\text{-}pum}$ $A1_{pum}$	167-NVPLDIAAMNS-177 to QVPLDLMAMNA	Undetectable
$CynD_{stut\text{-}pum}$ $A2_{pum}$	195-TASSHYAICNQA-206 to ISSRYYAIATQT	9.2 %±1.3 (0.021)
$CynD_{stut\text{-}pum}$ $C2_{pum}$	221-DMLCETQEEYFN-234 to EMICETQEQYFE	Undetectable

Proteins were expressed from non-induced constructs of pBC SK in MB3436 cells. The cyanide-degrading activity was measured by mixing 50 μl of overnight bacterial culture with 50 μl of 6 mM cyanide in 0.1 M MOPS, pH 7.7, and incubating at room temperature for 20 min. Residual cyanide was measured using picric acid. The results represent the average from three separate samples

was tested. Each of the six mutants remained active, but their activity differed (Fig. 3a). $CynD_{stut}$ G306A and D309A had only about 40–50 % of wild-type activity, $CynD_{stut}$ R308A retained about 60 % activity, and the other three mutants, E307A, S310A, and T311A, retained more than 80 % of wild-type activity.

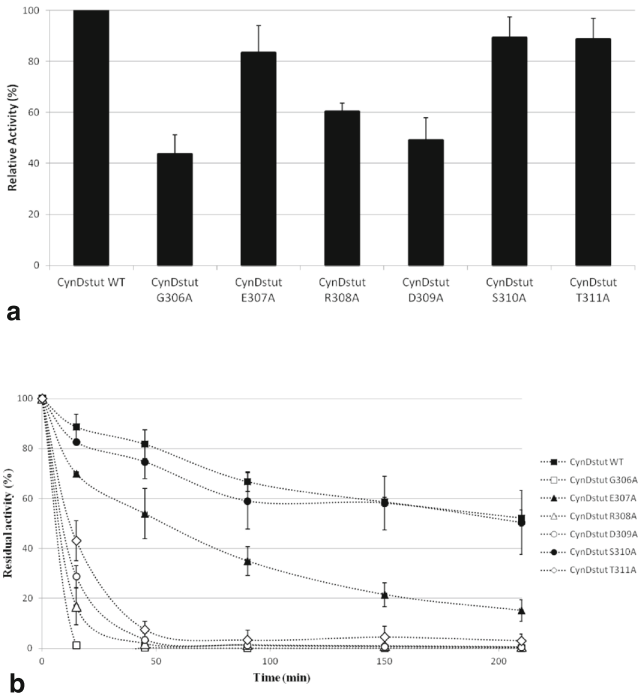

Fig. 3 Comparison of cyanide-degrading activity of $CynD_{stut}$ alanine mutants to the wild-type enzyme. **a** Relative activity as a percent of wild type was determined as in Fig. 2. **b** Thermostability of $CynD_{stut}$ alanine mutants. Cell lysates were incubated at 39 °C in a water bath, and the residual activity was tested at specified time points by detecting ammonia production. Activity at time 0 was considered 100 % for each mutant. *Error bars* indicate the standard deviation of the average from three experiments

The stability of these mutants was also probed by incubating cell lysates in 50 mM MOPS, pH 7.7, at 39 °C and testing the remaining activity after different times of incubation (Fig. 3b); $\Delta\Delta G$ values of these $CynD_{stut}$ mutants were subsequently computed using these data (Table 2). $CynD_{stut}$ G306A was highly unstable. It was completely inactivated within minutes and displayed a very negative $\Delta\Delta G$ of −11.9. Similarly, $CynD_{stut}$ R308A, $CynD_{stut}$ D309A, and $CynD_{stut}$ T311A were significantly reduced in stability; all three mutants lost 90 % of their activity after 45 min of incubation at 39 °C and displayed negative $\Delta\Delta G$ values of −8.7, −8.3, and −7.6 respectively . $CynD_{stut}$ E307A was similar but slightly less stable than wild type, losing 50 % of its activity after 1 h of incubation at 39 °C, conditions where the wild-type $CynD_{stut}$ lost 30 % of its activity. The S310A mutant was similar to wild type. $CynD_{stut}$ E307A and $CynD_{stut}$ S310A displayed negative $\Delta\Delta G$ value of −2.7 and −1.5, respectively, and although negative, these values were greater than those of $CynD_{stut}$ G306A, $CynD_{stut}$ R308A, $CynD_{stut}$ D309A, and $CynD_{stut}$ T311A.

Restoring the activity of $CynD_{stut\text{-}pum}$ hybrid

Using the inactive $CynD_{stut\text{-}pum}$ hybrid as a platform, the six residues in GERDST were investigated in various combinations by site-directed mutagenesis for restoration of activity to $CynD_{stut\text{-}pum}$.

The side chain charges of $CynD_{stut}$ and $CynD_{pum}$ at positions 307, 308, and 309 are reversed. $CynD_{stut}$ has a negative residue (E307) followed by a positive (R308) then a negative residue (D309). However, $CynD_{pum}$ has a positive residue (H307) then a neutral (Q308) and a positive residue (K309). If $CynD_{stut\text{-}pum}$ hybrid was inactive due to this inversion of charges in this important region, then mutationally reinstating the negative–positive–negative amino acids should restore the activity. This proved not to be true; $CynD_{stut\text{-}pum}$ 306NDKENE was inactive (Table 4).

Moving to the other residues in the essential 306GERDST region, the G306A mutation greatly affected both activity and stability of $CynD_{stut}$, suggesting its importance. Similar but lesser effects were seen for R308A, D309A, and somewhat for T311A. Therefore, the restoration of these residues in $CynD_{stut\text{-}pum}$ was conducted in combination with G306. Both $CynD_{stut\text{-}pum}$ *GHR*KN*T* or $CynD_{stut\text{-}pum}$ *GHQD*NE were inactive (Table 4).

Another residue, E307, also altered the stability of $CynD_{stut}$ when it was replaced by an alanine even though it had similar activity to wild type. Therefore, $CynD_{stut\text{-}pum}$ *GE*QKNE (N306G/H307E) was constructed. This mutant had some activity, about 15 % of wild-type $CynD_{stut}$ (Fig. 2) and only twofold less than $CynD_{stut\text{-}pum}$ GERDST. However, mutation H307E was unable to restore activity to the hybrid. These results indicate the importance of two residues in the $CynD_{stut}$ C-terminus, G306 and E307. In addition, other as yet

unknown residues outside the GERDST region of the C-terminus are required to restore full activity to the $CynD_{stut-pum}$ hybrid.

Identifying an interaction of the C-terminus with the A surface

The restoration of partial activity by substituting only a few residues in the C-terminus of $CynD_{stut-pum}$ raises the question whether mutations elsewhere in the protein could restore activity by repairing interactions with the C-terminus. Because the C-terminus has been seen interacting with both the A and C surfaces in structures of proteins from the larger superfamily (Kimani et al. 2007; Lundgren et al. 2008; Pace et al. 2000), four regions of CynD were predicted as possible participants in the oligomeric surfaces (Sewell et al. 2003; Sewell et al. 2005). These regions (from $CynD_{pum}$) were introduced individually into the inactive $CynD_{stut-pum}$ hybrid. Exchanging either of the C surface ($CynD_{stut-pum}$ $C1_{pum}$ and $CynD_{stut-pum}$ $C2_{pum}$) did not restore detectable activity. Similarly, the $CynD_{pum}$ A-surface region 167–177 (A1) had no effect on activity ($CynD_{stut-pum}$ $A1_{pum}$) (Table 5). However, $CynD_{stut-pum}$ carrying the *B. pumilus* A2 surface region 195–206 ($CynD_{stut-pum}$ $A2_{pum}$) did have partial activity (Table 5), although only about 10 % that of wild type $CynD_{stut}$ activity (Fig. 4). This result indicates that the $CynD_{pum}$ A2 region is able to partially suppress the disruptive effect of the $CynD_{pum}$ C-terminus in $CynD_{stut-pum}$.

Characterization of the A surface substitution

To test if the $CynD_{pum}$ A2 region was specific to the $CynD_{pum}$ C-terminus and not a general stability suppressor, it was also tested in the non-hybrid $CynD_{stut}$ background ($CynD_{stut}A2_{pum}$). $CynD_{stut}A2_{pum}$ did retain activity, but it was significantly lower (~16 %) than wild-type $CynD_{stut}$ (Fig. 4). Therefore, we cannot distinguish whether the 10 % activity of $CynD_{stut-pum}$ $A2_{pum}$ represents a very weak restoration of the C-terminus–A2 interaction or whether the restoration of the interaction is nearly complete but $CynD_{stut}$ is unable to tolerate the $A2_{pum}$ domain, and hence the 10 % activity is in the background of 16 % for its parent.

It was also tested whether the $CynD_{pum}$ A2 region made $CynD_{stut}$ tolerant to C-terminal deletions, similar to the $CynD_{pum}$ protein. $CynD_{pum}$ A2 region did not restore activity to deletion after residue 302 in $CynD_{stut}$ ($302CynD_{stut}\Delta302+A2_{pum}$) (Table 6), indicating that it does not remove the need for the C-terminal tail.

The A2 region is also not a determinant of the oligomer size difference between $CynD_{pum}$ and $CynD_{stut}$, which form 18 and 14 subunit oligomers, respectively (Jandhyala et al. 2003; Sewell et al. 2003). Size exclusion chromatography showed $CynD_{stut}A2_{pum}$ eluted with a profile similar to the wild-type $CynD_{stut}$ (data not shown). Similarly, the reverse hybrid $CynD_{pum-stut}$ migrated like $CynD_{pum}$, suggesting that neither A2 nor the C-terminus was itself determinant for oligomer size.

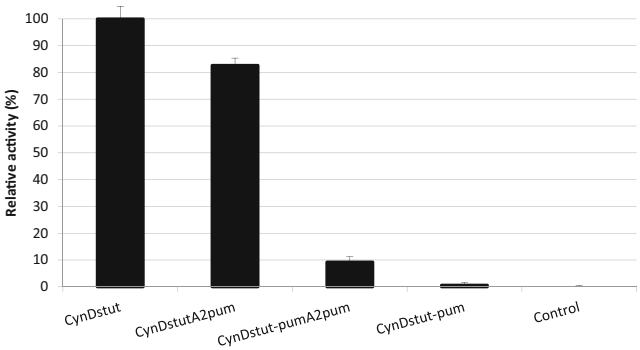

Fig. 4 Relative activity of A-surface region 2 (195–206) substitution mutants in $CynD_{stut}$ and $CynD_{stut-pum}$ compared to $CynD_{stut}$ and empty vector control. Cyanide degradation was monitored in whole cells using the picric acid assay. *Error bars* indicate the standard deviation from three independent cultures

Discussion

The cyanide dihydratases from *B. pumilus* and *P. stutzeri* share a very high level of sequence identity (80 %) over most of their amino acid sequence. This strong conservation remains, although at a lower level, when comparing cyanide dihydratases to cyanide hydratases such as from *N. crassa* and *G. sorghi*. However, in all cases, the C-termini are highly divergent both in sequence and in length (Basile et al. 2008). $CynD_{stut}$ has five additional residues relative to $CynD_{pum}$, and CHT_{sorghi} has an extension of ten carboxy terminal amino acids compared to CHT_{cras}. Even more striking is the divergence seen in the CynD proteins of two different but closely related *B. pumilus* strains, C1 and 8A3; out of only ten variant amino acids over the whole sequence, seven are found in the C-terminus (Jandhyala et al. 2003).

This divergence translates into differences in the properties of the protein. For example, $CynD_{pum}$ C1 formed long spirals

Table 6 The $CynD_{pum}$ A-surface region 195–206 does not act as a general stabilizer

Hybrid	Mutation	Activity
$CynD_{stut}$		100 %
$CynD_{stut}\Delta302$	Δ302	Undetectable
$CynD_{stut}\Delta302$ $+A2_{pum}$	Δ302 195TASS HYAICNQA206 to ISSRYYAIATQT (A2)	Undetectable

The activity was tested as in Table 5

at pH 5.4 instead of the 18-subunit short helix found at neutral pH (Jandhyala et al. 2003). However, $CynD_{pum}$ 8A3 does not undergo such transformation (Jandhyala et al. 2003). This reversible and pH-dependent structural change may be due to the protonation at pH 5.4 of the three histidines in the $CynD_{pum}$ C-terminus, H305, H308, and H323, whereas $CynD_{pum}$ 8A3 has none (Jandhyala et al. 2003). The positive charge on the histidines was proposed to lead to repulsion of the monomer C-terminus, expansion of the spiral's diameter, and elongation of the spiral. CHT_{cras} and $CynD_{stut}$ also do not show pH-dependent structural changes, keeping the same extended oligomers of variable length or 14 subunits, respectively (Dent et al. 2009; Sewell et al. 2003).

Another significant difference is seen in enzyme activity following truncation of the C-terminus. $CynD_{pum}$ is more tolerant to deletion than either $CynD_{stut}$ or CHT_{cras} (Table 1). With 28 carboxy terminal amino acids deleted, $CynD_{pum}$ Δ303 had a reaction rate comparable to wild type (Table 1), whereas $CynD_{stut}$ and CHT_{cras} were essentially inactivated by a similar deletion. This is not dissimilar to findings with the *Aspergillus niger* cyanide hydratase where deletion of the terminal 18 residues abolished activity (Rinagelova et al. 2014). Although $CynD_{pum}$ tolerates deletions in its C-terminus, they did have an effect on stability. The C-terminus may help stabilize the oligomeric structure of the enzyme, thereby suggesting that loss of activity with deletion might simply be the result of destabilizing the oligomeric structure.

The localization of the C-terminus in the folded protein is not yet clear. No structural data for this region are available due to the lack of sequence identity with closely related crystallographically determined structures, but it is thought that this domain is found in the center of the helix. This location was predicted based on distinct electron densities, observed on the inner surface of the oligomeric structures of bacterial nitrilases, in 3D reconstruction models (Sewell et al. 2003; Thuku et al. 2007) as well as the best fitting of homology models to the three-dimensional reconstructions of the nitrilases and cyanide hydratases.

Structural information from the known crystal structure of amidase might help predict the interfaces where the C-terminus could be interacting. Based on the visible C-terminal region of the amidase from *G. pallidus* (Kimani et al. 2007), Dent et al. (2009) have suggested that in *N. crassa* the C-terminus interacts with the C surface and then reaches across to the A surface. Similarly, in the C-shaped β-alanine synthase (βaS) from *D. melanogaster*, the C-terminus has interactions at both the A surface and C surface interfaces. Both of these surfaces are essential for oligomerization of the spiral and the activity of the nitrilase; thus, the role of the C-terminus may be to stabilize interactions at these interfaces.

Our result from substituting putative A- and C-surface regions in $CynD_{stut\text{-}pum}$ for the $CynD_{pum}$ sequences suggests a specific interaction of the *B. pumilus* C-terminus with the A-surface region 2 (195–206). Substituting the A2 region for the $CynD_{pum}$ sequence in $CynD_{stut\text{-}pum}$ ($CynD_{stut\text{-}pum}A2_{pum}$) restored partial activity (Fig. 4). Further, this region did not enhance the activity of the full-length $CynD_{stut}$ nor remove the need for the C-terminus altogether. The *B. pumilus* A2 region actually reduced activity in $CynD_{stut}$, suggesting specificity for the *B. pumilus* C-terminus. In crystal structures from the larger superfamily, the A surface is structurally linked to the positioning of the catalytic cysteine in the active site (Kumaran et al. 2003). The loss of activity in the $CynD_{stut}$ C-terminal deletions and $CynD_{stut\text{-}pum}$ hybrid may stem from loss of an interaction with the A surface. It is useful to note that Δ310 of *P. stutzeri*, which retains only minimal activity, carries the GERDS residues, although it is deleted for the final but not essential T311.

Neither the A surface interaction or the GERDST domain completely explains the incompatibility of the $CynD_{stut\text{-}pum}$ hybrid. Either region was only able to restore partial activity to $CynD_{stut\text{-}pum}$. $CynD_{stut\text{-}pum}$GERDST and $CynD_{stut\text{-}pum}A2_{pum}$ also had apparent defects in stability, with $CynD_{stut\text{-}pum}A2_{pum}$ not tolerating over-expression and $CynD_{stut\text{-}pum}$GERDST losing activity upon cell lysis. Other interactions between the C-terminus and the rest of the protein are unclear. The other oligomer surface regions and C-terminal segments examined did not restore detectable activity to $CynD_{stut\text{-}pum}$ when added individually. Another possibility comes from $CynD_{pum}$'s tolerance to C-terminal deletions. Perhaps the *B. pumilus* enzyme is inherently more stable than the *P. stutzeri* version and therefore does not require the C-terminus for activity. However, loss of the interaction between the C-terminus and the A surface could explain the drop in stability seen in $CynD_{pum}$Δ303.

A notable difference between $CynD_{stut}$ and $CynD_{pum}$ has been the size of their oligomers. $CynD_{stut}$ terminates at 14 subunits, while $CynD_{pum}$ extends to an 18-subunit oligomer (Jandhyala et al. 2003; Sewell et al. 2003). We tested if the A2 region was influencing the terminal size of the oligomer. The elution pattern of $CynD_{stut}A2_{pum}$ protein from size exclusion was consistent with the normal $CynD_{stut}$ 14 subunit oligomer, indicating that variation in self-termination stems from elsewhere in the protein. The oligomer size of $CynD_{stut\text{-}pum}$GERDST and $CynD_{stut\text{-}pum}A2_{pum}$ were not examined because the proteins did not survive cell lysis or over-expression.

Alterations to the C-terminal tail have been observed to affect activity and quaternary structure in both CynD and other nitrilases (Kiziak et al. 2007; Thuku et al. 2007; Wang et al. 2012), but a lack of clear conserved sequence or secondary structure has made it difficult to predict a common role in nitrilases (Thuku et al. 2009). Interactions between the C-terminal tail and the A surface are seen in multiple crystal structures of greatly diverged enzymes from the nitrilase superfamily. The interaction seen between these regions in CynD suggests that placement of the C-terminal tail at the A

surface may be common despite the sequence divergence seen in this region.

Acknowledgments The financial supports of The Welch Foundation (A1310) and the Texas Hazardous Waste Research Center are gratefully acknowledged.

Conflict of interest The authors declare that they have no conflict of interest.

References

Agarkar VB, Kimani SW, Cowan DA, Sayed MF, Sewell BT (2006) The quaternary structure of the amidase from *Geobacillus pallidus* RAPc8 is revealed by its crystal packing. Acta Crystallogr Sect F: Struct Biol Cryst Commun 62(Pt 12):1174–1178. doi:10.1107/S1744309106043855

Andrade J, Karmali A, Carrondo MA, Frazao C (2007a) Crystallization, diffraction data collection and preliminary crystallographic analysis of hexagonal crystals of *Pseudomonas aeruginosa* amidase. Acta Crystallogr Sect F: Struct Biol Cryst Commun 63(Pt 3):214–216. doi:10.1107/S1744309107005830

Andrade J, Karmali A, Carrondo MA, Frazao C (2007b) Structure of amidase from *Pseudomonas aeruginosa* showing a trapped acyl transfer reaction intermediate state. J Biol Chem 282(27):19598–19605. doi:10.1074/jbc.M701039200

Basile LJ, Willson RC, Sewell BT, Benedik MJ (2008) Genome mining of cyanide-degrading nitrilases from filamentous fungi. Appl Microbiol Biotechnol 80(3):427–435. doi:10.1007/s00253-008-1559-2

Dent KC, Weber BW, Benedik MJ, Sewell BT (2009) The cyanide hydratase from *Neurospora crassa* forms a helix which has a dimeric repeat. Appl Microbiol Biotechnol 82(2):271–278. doi:10.1007/s00253-008-1735-4

Hung CL, Liu JH, Chiu WC, Huang SW, Hwang JK, Wang WC (2007) Crystal structure of *Helicobacter pylori* formamidase AmiF reveals a cysteine–glutamate–lysine catalytic triad. J Biol Chem 282(16):12220–12229. doi:10.1074/jbc.M609134200

Jandhyala D, Berman M, Meyers PR, Sewell BT, Willson RC, Benedik MJ (2003) CynD, the cyanide dihydratase from *Bacillus pumilus*: gene cloning and structural studies. Appl Environ Microbiol 69(8):4794–4805

Jandhyala DM, Willson RC, Sewell BT, Benedik MJ (2005) Comparison of cyanide-degrading nitrilases. Appl Microbiol Biotechnol 68(3):327–335. doi:10.1007/s00253-005-1903-8

Kimani SW, Agarkar VB, Cowan DA, Sayed MF, Sewell BT (2007) Structure of an aliphatic amidase from *Geobacillus pallidus* RAPc8. Acta Crystallogr D Biol Crystallogr 63(Pt 10):1048–1058. doi:10.1107/S090744490703836X

Kiziak C, Klein J, Stolz A (2007) Influence of different carboxy-terminal mutations on the substrate-, reaction- and enantiospecificity of the arylacetonitrilase from *Pseudomonas fluorescens* EBC191. Protein Eng Des Sel 20(8):385–396. doi:10.1093/Protein/Gzm032

Kumaran D, Eswaramoorthy S, Gerchman SE, Kycia H, Studier FW, Swaminathan S (2003) Crystal structure of a putative CN hydrolase from yeast. Proteins Struct Funct Genet 52(2):283–291. doi:10.1002/Prot.10417

Lundgren S, Lohkamp B, Andersen B, Piskur J, Dobritzsch D (2008) The crystal structure of beta-alanine synthase from *Drosophila melanogaster* reveals a homooctameric helical turn-like assembly. J Mol Biol 377(5):1544–1559. doi:10.1016/j.jmb.2008.02.011

Meyers PR, Rawlings DE, Woods DR, Lindsey GG (1993) Isolation and characterization of a cyanide dihydratase from *Bacillus pumilus* C1. J Bacteriol 175(19):6105–6112

Nagasawa T, Wieser M, Nakamura T, Iwahara H, Yoshida T, Gekko K (2000) Nitrilase of *Rhodococcus rhodochrous* J1. Conversion into the active form by subunit association. Eur J Biochem 267(1):138–144

Nakai T, Hasegawa T, Yamashita E, Yamamoto M, Kumasaka T, Ueki T, Nanba H, Ikenaka Y, Takahashi S, Sato M, Tsukihara T (2000) Crystal structure of *N*-carbamyl-D-amino acid amidohydrolase with a novel catalytic framework common to amidohydrolases. Struct Fold Des 8(7):729–737. doi:10.1016/S0969-2126(00)00160-X

Nichols M, Willits C (1934) Reactions of Nessler's solution. J Am Chem Soc 56:769–774

Pace HC, Brenner C (2001) The nitrilase superfamily: classification, structure and function. Genome Biol 2(1):REVIEWS0001

Pace HC, Hodawadekar SC, Draganescu A, Huang J, Bieganowski P, Pekarsky Y, Croce CM, Brenner C (2000) Crystal structure of the worm NitFhit Rosetta Stone protein reveals a Nit tetramer binding two Fhit dimers. Curr Biol 10(15):907–917. doi:10.1016/S0960-9822(00)00621-7

Park J (2014) Regions involved in the oligomerization and activity of the spiral forming nitrilase Cyanide Dihydratase. Ph.D. Dissertation, Texas A&M University, USA

Rinagelova A, Kaplan O, Vesela AB, Chmatal M, Krenkova A, Plihal O, Pasquarelli F, Cantarella M, Martinkova L (2014) Cyanide hydratase from *Aspergillus niger* K10: overproduction in *Escherichia coli*, purification, characterization and use in continuous cyanide degradation. Process Biochem 49(3):445–450. doi:10.1016/J.Procbio.2013.12.008

Sewell BT, Berman MN, Meyers PR, Jandhyala D, Benedik MJ (2003) The cyanide degrading nitrilase from *Pseudomonas stutzeri* AK61 is a two-fold symmetric, 14-subunit spiral. Structure 11(11):1413–1422

Sewell BT, Thuku RN, Zhang X, Benedik MJ (2005) Oligomeric structure of nitrilases: effect of mutating interfacial residues on activity. Ann N Y Acad Sci 1056:153–159

Stevenson DE, Feng R, Dumas F, Groleau D, Mihoc A, Storer AC (1992) Mechanistic and structural studies on *Rhodococcus* ATCC 39484 nitrilase. Biotechnol Appl Biochem 15(3):283–302

Thimann KV, Mahadevan S (1964) Nitrilase. I. Occurrence preparation + general properties of enzyme. Arch Biochem Biophys 105(1):133. doi:10.1016/0003-9861(64)90244-9

Thuku RN, Brady D, Benedik MJ, Sewell BT (2009) Microbial nitrilases: versatile, spiral forming, industrial enzymes. J Appl Microbiol 106(3):703–727. doi:10.1111/j.1365-2672.2008.03941.x

Thuku RN, Weber BW, Varsani A, Sewell BT (2007) Post-translational cleavage of recombinantly expressed nitrilase from *Rhodococcus rhodochrous* J1 yields a stable, active helical form. FEBS J 274(8):2099–2108. doi:10.1111/j.1742-4658.2007.05752.x

Wang L, Watermeyer JM, Mulelu AE, Sewell BT, Benedik MJ (2012) Engineering pH-tolerant mutants of a cyanide dihydratase. Appl Microbiol Biotechnol 94(1):131–140. doi:10.1007/s00253-011-3620-9